THE JOURNAL OF BIOLOGICAL CHEMISTRY VOL. 285, NO. 51, pp. 40180–40191, December 17, 2010

Galantamine-induced Amyloid-β Clearance Mediated via Stimulation of Microglial Nicotinic Acetylcholine Receptors*[S]

Received for publication, May 7, 2010, and in revised form, September 22, 2010 Published, JBC Papers in Press, October 14, 2010, DOI 10.1074/jbc.M110.142356

Kazuyuki Takata[‡], Yoshihisa Kitamura[‡1,2], Mana Saeki[‡], Maki Terada[‡], Sachiko Kagitani[‡], Risa Kitamura[‡], Yasuhiro Fujikawa[‡], Alfred Maelicke[§], Hidekazu Tomimoto[¶], Takashi Taniguchi[‡], and Shun Shimohama[‖3]

From the [‡]Department of Neurobiology, Kyoto Pharmaceutical University, Misasagi, Yamashina-ku, Kyoto 607-8414, Japan, [§]Galantos Pharma GmbH, Freiligrathstrasse 12, 55131 Mainz, Germany, the [¶]Department of Neurology, Mie University, Graduate School of Medicine, Tsu 514-8507, Japan, and the [‖]Department of Neurology, Sapporo Medical University, School of Medicine, S1W16, Chuo-ku, Sapporo 060-8543, Japan

Reduction of brain amyloid-β (Aβ) has been proposed as a therapeutic target for Alzheimer disease (AD), and microglial Aβ phagocytosis is noted as an Aβ clearance system in brains. Galantamine is an acetylcholinesterase inhibitor approved for symptomatic treatment of AD. Galantamine also acts as an allosterically potentiating ligand (APL) for nicotinic acetylcholine receptors (nAChRs). APL-binding site is located close to but distinct from that for acetylcholine on nAChRs, and FK1 antibody specifically binds to the APL-binding site without interfering with the acetylcholine-binding site. We found that in human AD brain, microglia accumulated on Aβ deposits and expressed α7 nAChRs including the APL-binding site recognized with FK1 antibody. Treatment of rat microglia with galantamine significantly enhanced microglial Aβ phagocytosis, and acetylcholine competitive antagonists as well as FK1 antibody inhibited the enhancement. Thus, the galantamine-enhanced microglial Aβ phagocytosis required the combined actions of an acetylcholine competitive agonist and the APL for nAChRs. Indeed, depletion of choline, an acetylcholine-competitive α7 nAChR agonist, from the culture medium impeded the enhancement. Similarly, Ca^{2+} depletion or inhibition of the calmodulin-dependent pathways for the actin reorganization abolished the enhancement. These results suggest that galantamine sensitizes microglial α7 nAChRs to choline and induces Ca^{2+} influx into microglia. The Ca^{2+}-induced intracellular signaling cascades may then stimulate Aβ phagocytosis through the actin reorganization. We further demonstrated that galantamine treatment facilitated Aβ clearance in brains of rodent AD models. In conclusion, we propose a further advantage of galantamine in clinical AD treatment and microglial nAChRs as a new therapeutic target.

Alzheimer disease (AD)[4] is characterized by progressive cognitive impairment as a consequence of extensive neuronal loss (1). Pathological hallmarks of AD include the development of senile plaques by the accumulation of extracellular amyloid-β (Aβ) and neurofibrillary tangles formed by intraneuronal accumulation of hyperphosphorylated tau. According to the amyloid hypothesis, accumulation of Aβ in the brain parenchyma is the primary event influencing other AD pathologies such as the formation of neurofibrillary tangles and neuronal cell death (2). Therefore, reduction of brain Aβ has been proposed as a primary therapeutic target for AD. In mouse models of AD, active immunization with Aβ peptides reduced brain Aβ and restored cognitive functions (3–5). One proposed mechanism of this Aβ reduction is the promotion of microglial Aβ phagocytosis via Fc receptors (6, 7). A case report of an Aβ immunization clinical trial also suggested the contribution of microglia in Aβ clearance (8).

Deficits of cholinergic function have been demonstrated in AD brain (9–12). These findings provide the rationale for cholinergic enhancement as an approach to improve cognitive function in AD, and acetylcholinesterase (AChE) inhibitors are currently approved for AD treatment. Their therapeutic benefits are commonly regarded as purely symptomatic, and they are considered only a partial answer for AD treatment. However, most of them exhibit effects that are inconsistent with purely symptomatic actions, and it has been suggested that some AChE inhibitors induce molecular and cellular changes that directly influence AD pathologies.

Galantamine is a centrally acting AChE inhibitor. Although its AChE inhibitory activity appears to be much weaker than other clinically available AChE inhibitors, its therapeutic effects on cognitive function in AD are comparable with the other agents (13–15). Furthermore, the latest long term ex-

* This work was supported in part by Frontier Research Program, grants-in-aid from the Ministry of Education, Culture, Sports, Science and Technology of Japan, and the Japan Society for Promotion of Science.

[S] The on-line version of this article (available at http://www.jbc.org) contains supplemental Videos S1–S3.

[1] Both authors contributed equally to this work.

[2] To whom correspondence may be addressed: Dept. of Neurobiology, Kyoto Pharmaceutical University, Misasagi, Yamashina-ku, Kyoto 607-8414, Japan. Tel.: 81-75-595-4706; Fax: 81-75-595-4796; E-mail: yo-kita@mb.kyoto-phu.ac.jp.

[3] To whom correspondence may be addressed: Dept. of Neurology, Sapporo Medical University, School of Medicine, S1W16, Chuo-ku, Sapporo 060-8543, Japan. Tel.: 81-11-611-2111, Ext. 3820; Fax: 81-11-622-7668; E-mail: shimoha@sapmed.ac.jp.

[4] The abbreviations used are: AD, Alzheimer disease; Aβ, amyloid-β; Aβ42, Aβ1–42; AChE, acetylcholinesterase; α7 nAChR, α7 subunit of nAChR; APL, allosterically potentiating ligand; Ca^{2+} (−) DMEM, Ca^{2+}-free DMEM; Ca^{2+} (+) DMEM, Ca^{2+}-free DMEM supplemented with 1.8 mM Ca^{2+}; CaM, calmodulin; CaMKII, Ca^{2+}/CaM-dependent protein kinase II; choline (−), choline-free; choline (+) DMEM, choline (−) DMEM supplemented with 28 μM choline; FA, formic acid; FSB, 1-fluoro-2,5-bis(3-carboxy-4-hydroxystyryl)benzene; Iba1, ionized calcium binding adaptor molecule 1; JAK2, Janus activated kinase-2; MAPKK, mitogen-activated protein kinase kinase; MLA, methyllycaconitine; nAChR, nicotinic acetylcholine receptor; PI3K, phosphoinositide-3 kinase; Rac1, Ras-related C3 botulinum toxin substrate 1; TBS, Tris-buffered saline; MWM, Morris water maze; WAVE, Wiskott-Aldrich syndrome protein family verprolin-homologous protein.

tension clinical trial of galantamine suggested that the cognitive benefits of galantamine are sustained for at least 36 months (16). Several lines of evidence suggest that the therapeutic effects of galantamine are mediated by additional mechanisms apart from AChE inhibition. Galantamine actually acts as an allosterically potentiating ligand (APL) for nicotinic acetylcholine receptors (nAChRs) (17–20) and exhibits neuroprotective effects *in vitro* (21) and *in vivo* (22).

A recent study has shown that microglia express the α7 subunit of nAChRs (α7 nAChRs) (23) and that treatment with nicotine modulates secretion of tumor necrosis factor from microglia, resulting in neuroprotection (24). It therefore seems feasible that galantamine acts as an APL on microglial nAChRs to modulate microglial function. In the present study, we examined the effect of galantamine on microglial Aβ phagocytosis.

EXPERIMENTAL PROCEDURES

Reagents—Reagents and their sources included the following: DMEM and Ca^{2+}-free [Ca^{2+} (−)] DMEM from Invitrogen; nicotine, mecamylamine, methyllycaconitine (MLA), atropine, AG490, PD98059, choline, and Toxin B from Sigma; galantamine hydrobromide from Tocris; synthetic human Aβ1–42 (Aβ42) from AnaSpec; W-7 from Biomol International; choline-free (choline (−)) DMEM from Nikken Biomedical Laboratory; 1-fluoro-2,5-bis(3-carboxy-4-hydroxystyryl)benzene (FSB) and Fluo 4-AM from Dojindo; Hoechst 33258 and rhodamine-conjugated phalloidin from Invitrogen; and KN-93, PP2, LY294002, and NSC23766 from Calbiochem. The primary antibodies used in this study were antibodies against α7 nAChR (clone 306; Sigma), Aβ42 (clone 82E1; IBL), and ionized calcium-binding adaptor molecule 1 (Iba1; Wako). Monoclonal antibody FK1 was raised against membrane preparation from hindleg muscles of newborn rats as described previously (25, 26). All other regents were purchased from commercial sources and were of the highest purity available.

Human Materials and Preparation of Brain Sections—All of the experiments using human materials were performed in accordance with the guidelines of Kyoto Pharmaceutical University Ethical Committee. Informed consent was obtained from the subject. The tissues of frontal cortices from a patient who was clinically and histopathologically diagnosed as having AD (67 years of age; Consortium to Establish a Registry for Alzheimer's Disease criteria C; Braak stage IV) were used. The dissected tissue blocks were fixed in 10% formalin and then were cut into 20-μm sections on a cryostat.

Rat Microglial Culture—Primary-cultured rat microglia were prepared as previously described (7, 27, 28). Forebrains from newborn Wistar rats were minced and filtrated through a 70-μm-diameter nylon mesh. The cells were cultured in DMEM with 10% fetal bovine serum at 37 °C in humidified 5% CO_2, 95% air. At 21 days, floating microglia were isolated from the cell cultures. Purified microglia were treated with Aβ42 alone or simultaneously with galantamine and/or nicotine. Antagonists or inhibitors were added individually to microglia 10 min prior to treatment with Aβ42.

Rodent Models of AD and Drug Treatment—All of the animal experiments were carried out in accordance with the National Institutes of Health Guide for the Care and Use of Laboratory Animals, and the protocols were approved by the Committee for Animal Research at Kyoto Pharmaceutical University. The rats were anesthetized with sodium pentobarbital, and 1 μg of human Aβ42 was injected into the hippocampus as previously described (29). Starting the day after the Aβ42 injection, the rats received 1 or 5 mg/kg of galantamine or 1 ml/kg of PBS intraperitoneally once daily for 2 weeks. On the day after the final drug treatment, the hippocampus was dissected and was prepared for ELISA as described below.

Hemizygous APdE9 mice expressing chimeric mouse/human amyloid precursor protein APPswe (mouse APP695 harboring a human Aβ domain and mutations K594N and M595L linked to Swedish familial AD pedigrees) and human mutated presenilin 1-dE9 (deletion of exon 9) were purchased from Jackson Laboratory (30). Starting at 9 months of age, groups of APdE9 mice were orally administrated 1 mg/kg ($n = 7$) or 5 mg/kg ($n = 7$) of galantamine or 10 ml/kg of PBS ($n = 7$) once daily for 2 months (56 days). Groups of age-matched nontransgenic littermates received 5 mg/kg of galantamine ($n = 7$) or 10 ml/kg of PBS ($n = 7$). On the day after the final drug treatment, the mice were killed by cervical dislocation, and the brains were removed. One cerebral hemisphere was prepared for ELISA as described below, and the other was post-fixed in 4% paraformaldehyde for histochemical analysis.

Immunohistochemical Analysis—Free-floating brain sections of human AD and APdE9 mice were co-incubated with anti-Iba1 antibody (diluted 1:1,000) and anti-α7 nAChR antibody (1:100) or with anti-Iba1 antibody and FK1 antibody (1:50). The brain sections were further incubated with FSB (1:50). Primary-cultured rat microglia were fixed with 4% paraformaldehyde and then incubated with anti-Aβ antibody (1:3,000), anti-α7 nAChR antibody (1:500), or FK1 antibody (1:50). The rat microglia were also incubated with rhodamine-conjugated phalloidin (1:40) and Hoechst 33258 (1:5,000). The brain sections and primary-cultured rat microglia were then probed with Alexa Fluor-labeled secondary antibodies (each diluted 1:500) as appropriate. Subsequently, fluorescence was scanned using a laser confocal microscope (LSM510META; Carl Zeiss).

The brain sections of APdE9 mice were also incubated with anti-Aβ antibody (1:3,000). The sections were then incubated with biotinylated anti-mouse IgG antibody (1:2,000; Vector Laboratories) and followed by the incubation with avidin peroxidase (ABC Elite kit; 1:4,000; Vector Laboratories). Subsequently, the labeling was visualized by incubation with 50 mM Tris-HCl buffer (pH 7.6) containing 0.02% 3,3′-diaminobenzidine and 0.0045% hydrogen peroxide with nickel enhancement.

Time Lapse Imaging Assay—In the time lapse imaging assay for Ca^{2+}, primary-cultured rat microglia were incubated with Fluo 4-AM in Ca^{2+} (−) DMEM, and then the culture medium was replaced with Ca^{2+} (−) DMEM supplemented with 1.8 mM Ca^{2+} (Ca^{2+} (+) DMEM). Fluorescence of Fluo 4 was monitored at a rate of 1 scan/s using LSM510META. In the

middle of the laser scanning, a drop of concentrated galantamine or nicotine was added to obtain a final concentration of 1 μM galantamine or 1 mM nicotine, respectively. Subsequently, the images were reconstructed into supplemental videos using the software iMovie (Apple Inc.).

Biochemical Analysis—Western blot analysis was performed as previously described (7, 27, 28) using anti-α7 nAChR antibody (1:1,000) or FK1 antibody (1:5,000). The amounts of Aβ phagocytosed by rat microglia and those in the brains of Aβ-injected rats and APdE9 mice were measured by ELISA. Briefly, at 12 h after the treatment of Aβ42 to rat microglia, culture medium was collected. The rat microglia were rinsed with PBS and then lysed with PBS containing 0.1% Triton X-100. The brains of Aβ-injected rats and APdE9 mice were homogenized with Tris-buffered saline (TBS). The homogenate was centrifuged at 100,000 × *g* for 1 h, and the supernatant was collected as the TBS-extracted fraction. 70% formic acid (FA) was added to the pellet, which was homogenized again. The homogenate was incubated for 1 h at 4 °C and then centrifuged at 100,000 × *g* for 1 h at 4 °C. The resultant supernatant was collected as the FA-extracted fraction, which was neutralized with a 20-fold volume of 1 M Tris buffer (pH 11.0). Subsequently, the amounts of Aβ in the culture medium, cell lysate, TBS-extracted fraction, and neutralized FA-extracted fraction were measured using a human Aβ42 or Aβ40 specific ELISA kit (IBL) according to the manufacturer's instructions.

RT-PCR—Total microglial RNA was extracted using the Isogene RNA isolation kit (Nippon Gene), and first strand cDNA was synthesized using a RT-PCR kit (GE Healthcare) according to the manufacturer's instructions. Second strand cDNA synthesis/PCR amplification was performed with α7 nAChR subunit-specific primer set (forward, 5′-TTT CTG CGC ATG AAG AGG CCC GGA GAT-3′ and reverse, 5′-ACC TCC TCC AGG ATC TT-3′). PCR products were electrophoresed on 2% agarose gels and stained with ethidium bromide.

Water Maze Testing—Morris water maze (MWM) examination was performed in a circular pool (diameter, 120 cm; height, 30 cm). The pool was filled with water (maintained at 25.0 ± 1.0 °C) and was located in a large room with various distal visual cues. An invisible (transparent) circular platform (diameter, 10 cm) was submerged ~1.0 cm below the surface of the water and placed in the center of the south quadrant. The swimming activity of each mouse was monitored via a video camera mounted overhead, which relayed information including latency to find the platform, total distance traveled, and time and distance spent in each quadrant to a video tracking system (Muromachi). Each mouse was given three acquisition trials/day for 3 consecutive days to locate and climb on to the hidden platform. An acquisition trial was initiated by placing the mouse in the water with its nose directly facing the pool wall. The starting position varied between five constant locations at the pool rim. For each trial, the mouse was allowed to swim a maximum of 120 s to find the platform. When successful, the mouse was allowed a 30-s rest period on the platform. If unsuccessful within the allotted time period, the mouse was given a score of 120 s and then physically placed on the platform and also allowed the 30-s rest period. One day following the last acquisition trial, a single probe test was conducted for each study subject to measure spatial bias for previous platform location. This was accomplished by removing the platform from the pool and measuring the time spent in the previous platform quadrant location for 100 s. Starting 4 days and 3 days before the first and final drug treatment, respectively, each mouse was given two sets of the MWM examination.

Statistical Evaluation—All of the data represent the means ± S.E. In the ELISA, the statistical significance of differences among groups was determined by an analysis of variance with a Bonferroni/Dunn test. In the MWM, the mean sources during acquisition trials were analyzed using two-way repeated measures analysis of variance, with genotype and the test day of acquisition trials or treatment group and the test day of acquisition trials as sources of variation. As the multiple comparison among APdE9 mice treated with vehicle and galantamine (1 and 5 mg/kg), Fisher's protected least significant difference (Fisher's PLSD) test was used to examine post hoc differences. In probe tests, the search bias in the target quadrant was compared between vehicle-treated nontransgenic littermates and vehicle-treated APdE9 mice by using Student's *t* test. The search bias among APdE9 mice treated with vehicle and galantamine (1 and 5 mg/kg) was evaluated by an analysis of variance with a Bonferroni/Dunn test.

RESULTS

Expression of α7 nAChRs in Human AD Brain and Rat Microglia—We first analyzed the expression of nAChRs on microglia in human AD brain. Microglia labeled with anti-Iba1 antibody (Fig. 1*B*) accumulated on the Aβ plaque probed with FSB (Fig. 1*A*), an Aβ-binding fluorescent dye. The immunoreactivities of α7 nAChRs (Fig. 1*C*) were co-localized with the microglia (Fig. 1*D*, *arrows*).

We next prepared primary cultures of rat microglia, which expressed the mRNA of α7 nAChRs (Fig. 1*E*). In Western blot analysis, we also detected the protein of α7 nAChRs in rat microglia with primary cultures of rat neuron (21) and rat liver homogenate (31) as positive and negative controls, respectively (Fig. 1*F*). In laser confocal microscopic analysis, immunoreactivity of α7 nAChRs (Fig. 1*H*) was detected in rod-shaped rat microglia (Fig. 1*G*), and the merged image (Fig. 1*I*) showed that they were strongly expressed on the microglial cell surface.

Enhancement of Rat Microglial Aβ Phagocytosis by Galantamine—In previous studies, we reported that primary-cultured rat microglia markedly phagocytose Aβ (7, 27, 28). In the present study, we treated rat microglia with 1 μM Aβ42 in the presence or absence of galantamine or nicotine. The amount of Aβ phagocytosed by microglia was then measured by ELISA at 12 h after treatment. Galantamine enhanced microglial Aβ phagocytosis in a concentration-dependent manner, and phagocytosis reached the maximum at 1 μM galantamine (Fig. 2*A*). Similarly, nicotine, a classical acetylcholine competitive agonist, increased microglial Aβ phagocytosis, and the phagocytosis was significantly enhanced by treatment with 1,000 μM nicotine (Fig. 2*B*).

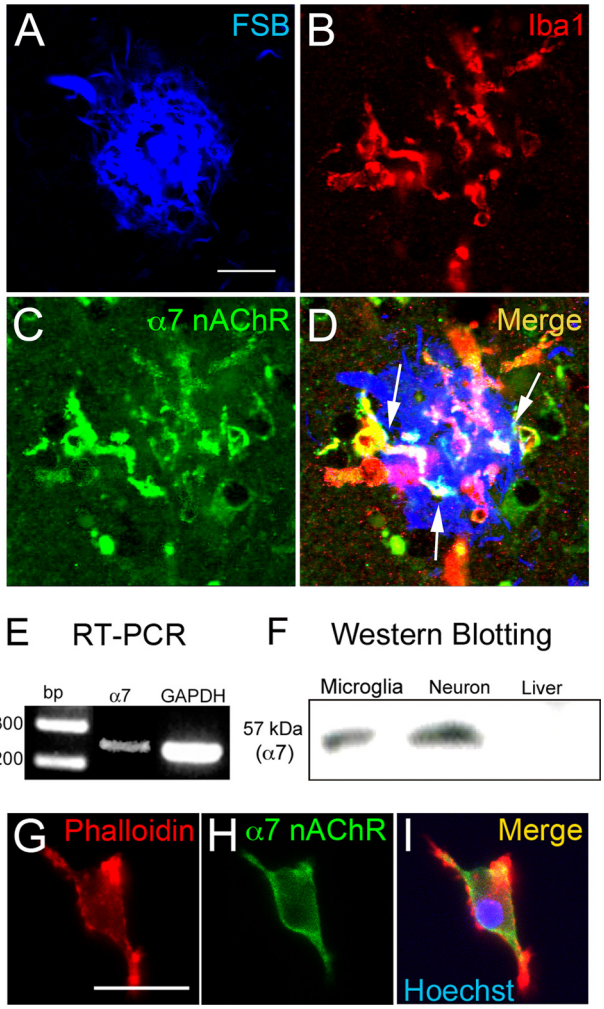

FIGURE 1. **α7 nAChRs in human AD brain and on primary-cultured rat microglia.** *A–D*, in the AD brain, immunoreactivities of α7 nAChRs (*C*, green) were co-localized (*D*, *arrows*) with microglia (*B*, Iba1; *red*) accumulated on Aβ plaque (*A*, FSB; *blue*). *Scale bar*, 20 μm. *E*, RT-PCR demonstrated the expression of mRNA of α7 nAChRs in rat microglia. *F*, in Western blot analysis, proteins of α7 nAChRs were detected in rat microglia and neurons but not in rat liver. α7, α7 nAChRs. *G–I*, rhodamine-conjugated phalloidin, a fluorescent probe for actin cytoskeleton, revealed the rod-shaped rat microglia (*G*, *red*). α7 nAChR (*H*, *green*) was expressed on the microglia (*I*). In *I*, the *blue area* indicates microglial nucleus labeled with Hoechst 33258. *Scale bar*, 20 μm.

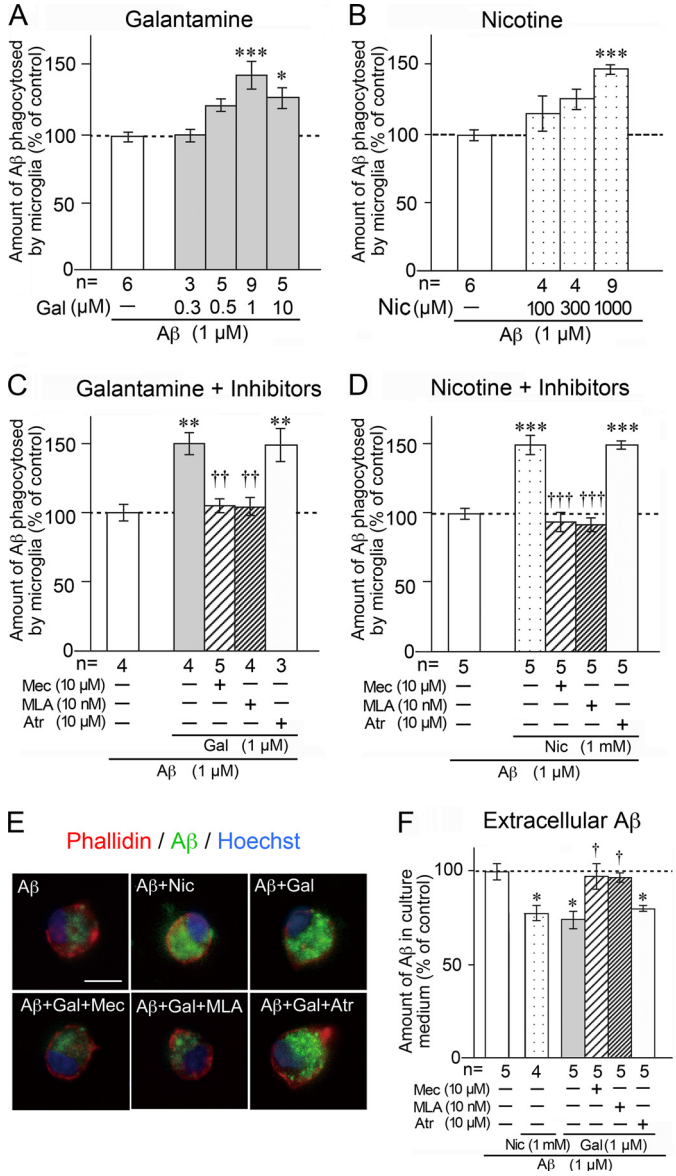

FIGURE 2. **Enhancement of microglial Aβ phagocytosis by galantamine or nicotine.** The amount of Aβ phagocytosed by rat microglia was measured by ELISA after treatment with 1 μM Aβ42 for 12 h in the presence or absence of galantamine (*A*) or nicotine (*B*). Pretreatment with mecamylamine, methyllycaconitine, or atropine was done for 10 min before the addition of galantamine (*C*) or nicotine (*D*). *E*, microglial actin cytoskeleton (*red*), nucleus (*blue*), and phagocytosed Aβ (*green*) were detected in laser confocal microscopic analysis. *Scale bar*, 10 μm. *F*, amount of extracellular Aβ in the culture medium was measured by ELISA. *, $p < 0.05$; **, $p < 0.01$; ***, $p < 0.001$ *versus* Aβ42 alone (*A–D* and *F*). †, $p < 0.05$; ††, $p < 0.01$; †††, $p < 0.001$ *versus* Aβ42 plus galantamine (*C* and *F*) or nicotine (*D*). *Gal*, galantamine; *Nic*, nicotine; *Mec*, mecamylamine; *Atr*, atropine; *n*, number of samples.

Microglia were next pretreated with acetylcholine competitive nAChR antagonists. Pretreatment with mecamylamine (a nonselective nAChR antagonist) or MLA (an α7 nAChR-specific antagonist) prevented the galantamine-enhanced (Fig. 2*C*) or nicotine-enhanced (Fig. 2*D*) microglial Aβ phagocytosis. In contrast, atropine, a muscarinic AChR antagonist, did not inhibit the enhanced phagocytosis (Fig. 2, *C* and *D*). Confocal microscopic analysis supported this result (Fig. 2*E*). In the presence of Aβ, microglia changed from rod-shaped (Fig. 1*G*) to round amoeboid-shaped (Fig. 2*E*, *red*) morphology and markedly phagocytosed Aβ (Fig. 2*E*, *green*). Treatment with galantamine increased the intensity of Aβ inside microglia, and this increase was inhibited by pretreatment with mecamylamine or MLA, but not with atropine. We subsequently measured the amount of extracellular Aβ in microglial culture medium (Fig. 2*F*). Extracellular Aβ amounts were significantly reduced by simultaneous treatment with galantamine plus Aβ or nicotine plus Aβ, and the reductions were inhibited by pretreatment with mecamylamine or MLA, but not with atropine. Thus, we found that microglial Aβ phagocytosis is enhanced by galantamine or nicotine, at least in part through α7 nAChRs.

Expression of APL-binding Site for nAChRs in Human AD Brain and Rat Microglia—Galantamine acts as an APL for nAChRs (17–20). The APL-binding site is located close to but distinct from that for acetylcholine on nAChRs, and FK1 anti-

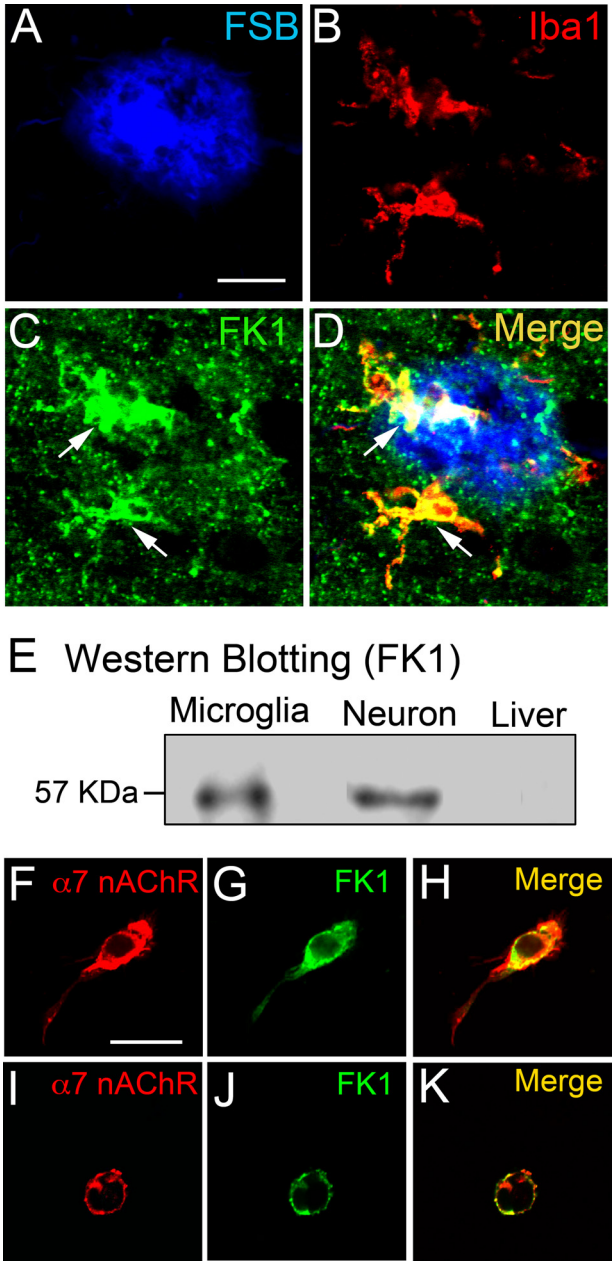

FIGURE 3. **APL-binding site for nAChRs in human AD brain and on primary-cultured rat microglia.** *A–D*, in the AD brain, several intense immunoreactivities of APL-binding site for nAChRs (*C*, FK1; *green*, *arrows*) were co-localized (*D*, *arrows*) with microglia (*B*, Iba1; *red*) accumulated on Aβ plaque (*A*, FSB; *blue*). *Scale bar*, 20 μm. *E*, in Western blot analysis, proteins of the APL-binding site for nAChRs were detected in rat microglia and neurons but not in rat liver. *F–K*, confocal microscopic analysis revealed that α7 nAChRs (*F* and *I*; *red*) were co-localized (*H* and *K*) with the APL-binding site for nAChRs (*G* and *J*; *green*) on both resting rod-shaped rat microglia (*F–H*) and phagocytic amoeboid-shaped rat microglia treated with 1 μM Aβ42 (*I–K*). *Scale bar*, 20 μm.

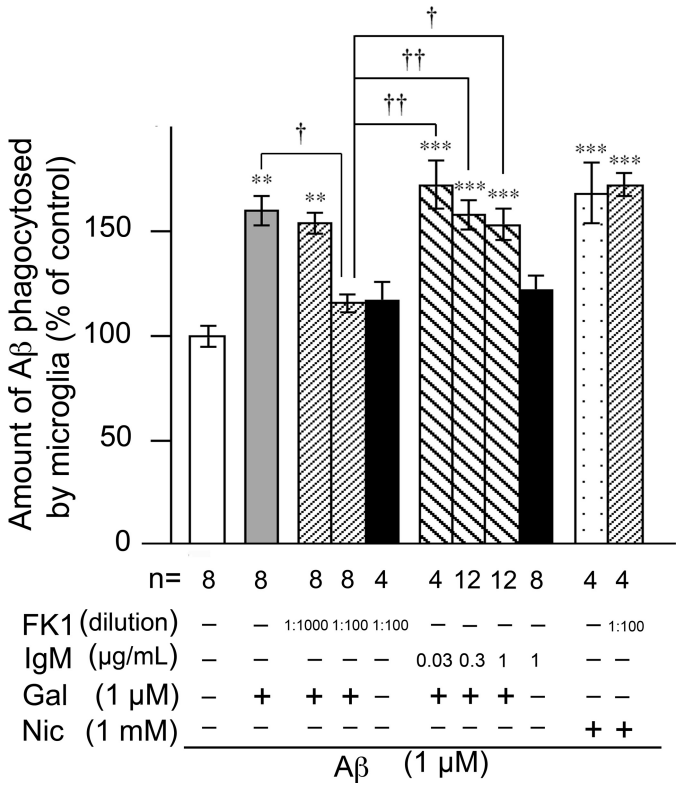

FIGURE 4. **Involvement of the APL-binding site for nAChRs in galantamine-enhanced microglial Aβ phagocytosis.** Rat microglia was treated with 1 μM Aβ42 in the presence or absence of 1 μM galantamine or 1 mM nicotine. FK1 antibody or mouse IgM isotype control was added 10 min before treatment of Aβ42. The amounts of Aβ phagocytosed by microglia were measured by ELISA. **, $p < 0.01$; ***, $p < 0.001$ *versus* Aβ42 alone. †, $p < 0.05$; ††, $p < 0.01$ *versus* Aβ42 plus galantamine and FK1 antibody (1:100). *FK1*, FK1 antibody; *IgM*, mouse IgM isotype control; *Gal*, galantamine; *Nic*, nicotine; *n*, number of samples.

body specifically binds to the APL-binding site without interfering with the acetylcholine-binding site (25, 26). Therefore, we next analyzed expression of the APL-binding site for nAChRs using the FK1 antibody in human AD brain. The Aβ plaque (Fig. 3*A*) and activated microglia (Fig. 3*B*) were probed with FSB and anti-Iba1 antibody, respectively. Immunoreactivity of APL-binding sites appeared as dot-like areas throughout the AD brain parenchyma (Fig. 3*C*), and areas of intense immunoreactivity were also observed (Fig. 3*C*, *arrows*). A merged image (Fig. 3*D*) revealed that areas with strong immunoreactivity to FK1 antibody were co-localized with the microglia accumulated on the Aβ plaque in human AD brain (Fig. 3*D*, *arrows*).

In Western blot analysis using FK1 antibody, we detected expression of the APL-binding site for nAChRs in primary cultures of rat microglia and neurons, but not in rat liver (Fig. 3*E*). We further confirmed the co-localization of α7 nAChRs and APL-binding sites in the rod-shaped untreated microglia (Fig. 3, *F–H*) and amoeboid-shaped Aβ-treated microglia (Fig. 3, *I–K*) by laser confocal microscopy.

APL-binding Site for nAChRs in Galantamine-enhanced Aβ Phagocytosis—Using FK1 antibody, we examined the involvement of the APL-binding site in galantamine- or nicotine-enhanced microglial Aβ phagocytosis (Fig. 4). Because FK1 antibody is a mouse IgM antibody, the treatment with mouse IgM isotype control (Sigma) instead of FK1 antibody was included as a negative control. Although galantamine-enhanced microglial Aβ phagocytosis was significantly inhibited by FK1 antibody (1:100, ~1 μg/ml IgM), FK1 antibody alone did not influence the magnitude of Aβ phagocytosis in the absence of galantamine. Mouse IgM isotype control had no inhibitory effects on galantamine-enhanced Aβ phagocytosis or on Aβ phagocytosis in the absence of galantamine. Thus, FK1 anti-

body abolished galantamine-enhanced microglial Aβ phagocytosis. However, treatment with FK1 antibody (1:100) did not inhibit nicotine-enhanced Aβ phagocytosis. These results suggest that galantamine enhances microglial Aβ phagocytosis by acting on the APL-binding site for nAChRs, whereas nicotine increases phagocytosis by directly interacting with the acetylcholine-binding site.

Requirement of Choline for Galantamine-enhanced Aβ Phagocytosis—APLs interact with a binding site on nAChRs that is distinct from the acetylcholine-binding site, and from there APLs sensitize nAChRs to respond to acetylcholine or acetylcholine competitive agonists (19, 32). Thus, APLs act as modulatory ligands for nAChRs rather than as agonists. In this context, galantamine may need acetylcholine or some acetylcholine competitive agonists to induce activation of microglial nAChRs. In fact, MLA, the acetylcholine competitive antagonist for α7 nAChRs, inhibited galantamine-enhanced microglial *Aβ* phagocytosis (Fig. 2*C*). Therefore, we checked whether our microglial culture medium contained acetylcholine or acetylcholine competitive agonists and found 28 μM choline. Choline functions as a relatively selective and competitive agonist for the acetylcholine-binding site on α7 nAChRs (33–35). Therefore, we next examined how choline affected microglial Aβ phagocytosis in the presence or absence of galantamine (Fig. 5, *A* and *B*). In the absence of galantamine, the levels of microglial Aβ phagocytosis were almost the same in choline (−) DMEM and choline (−) DMEM supplemented with 28 μM choline [choline (+) DMEM] (Fig. 5*A*). However, enhanced Aβ phagocytosis induced by galantamine in choline (+) DMEM was abolished in choline (−) DMEM. In contrast, microglial Aβ phagocytosis was enhanced by nicotine in a choline-independent manner.

We further examined concentration-dependent effects of choline and nicotine on microglial Aβ phagocytosis (Fig. 5, *B* and *C*, respectively). In the absence of galantamine, choline and nicotine (both 100 μM-1 mM) increased Aβ phagocytosis in a concentration-dependent manner, and the response peaked at 1 mM choline and nicotine. In contrast, in the presence of galantamine, phagocytosis was increased already at 1 μM choline or 0.03 μM nicotine and peaked at 10 μM choline or 1 μM nicotine. These results suggest that choline acts as an acetylcholine competitive agonist for microglial nAChRs and enhances Aβ phagocytosis. Thus, we found that galantamine dramatically sensitizes microglial nAChRs to choline and nicotine.

Ca^{2+} Influx and Calmodulin-dependent Pathway in Galantamine-enhanced Aβ Phagocytosis—The α7 nAChRs are known to function as ligand-gated Ca^{2+} channels (36). To test for this activity in microglia, a time lapse Ca^{2+} imaging study using Fluo 4-AM, a Ca^{2+}-sensitive fluorescent dye, was conducted in the choline (+) DMEM (Fig. 6*A* and supplemental Videos S1–S3). Faint Fluo 4 fluorescence was observed in resting rat microglia before drug treatment. Vehicle treatment did not influence the intensity of Fluo 4 fluorescence (Fig. 6*A*, *top panels*, and supplemental Video S1). On the other hand, Fluo 4 fluorescence was increased transiently in the microglial cytoplasm ~30 s after the addition of galantamine (Fig. 6*A*, *middle panels*, and supplemental Video S2) or nicotine (Fig. 6*A*, *bottom panels*, and supplemental Video S3) and returned to the basal level within ~1 min. These results suggest that nAChRs in microglia indeed function as Ca^{2+} channels.

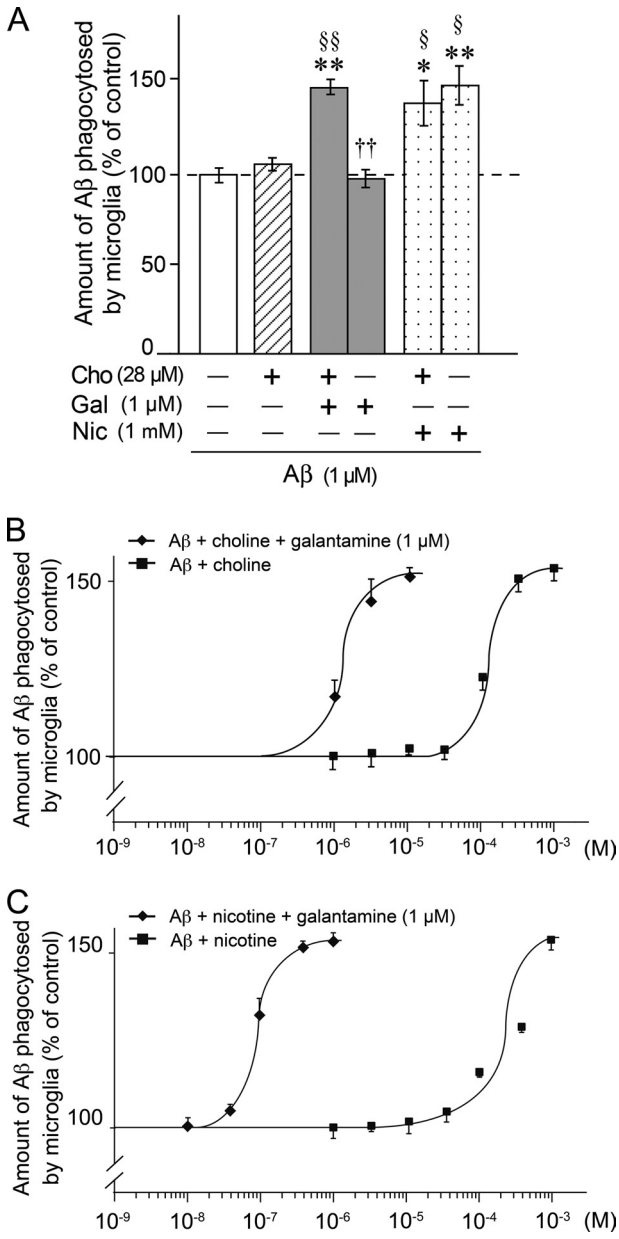

FIGURE 5. **Involvement of choline in galantamine-enhanced microglial Aβ phagocytosis.** *A*, rat microglia were cultured in the presence or absence of 28 μM choline and treated with 1 μM Aβ42 plus 1 μM galantamine, or 1 μM Aβ42 plus 1 mM nicotine. The amount of Aβ42 phagocytosed by microglia was measured by ELISA. *, $p < 0.05$; **, $p < 0.01$ *versus* Aβ42 alone in choline-free culture medium. §, $p < 0.05$; §§, $p < 0.01$ *versus* Aβ42 alone in choline-containing culture medium. ††, $p < 0.01$ *versus* Aβ42 plus galantamine in choline-containing culture medium. *Cho*, choline; *Gal*, galantamine; *Nic*, nicotine. The data represent the means ± S.E. of seven samples in each group. *B*, concentration-dependent curves of the choline effect on microglial Aβ phagocytosis were investigated. The data represent the means ± S.E. of 4–13 samples in each group. *C*, concentration-dependent curves of the nicotine effect on microglial Aβ phagocytosis were investigated in the absence of choline. The data represent the means ± S.E. of 3–7 samples in each group.

We next investigated whether the Ca^{2+} influx correlates with enhanced microglial Aβ phagocytosis. In this assay, we used Ca^{2+} (−) DMEM containing 28 μM choline and cap-

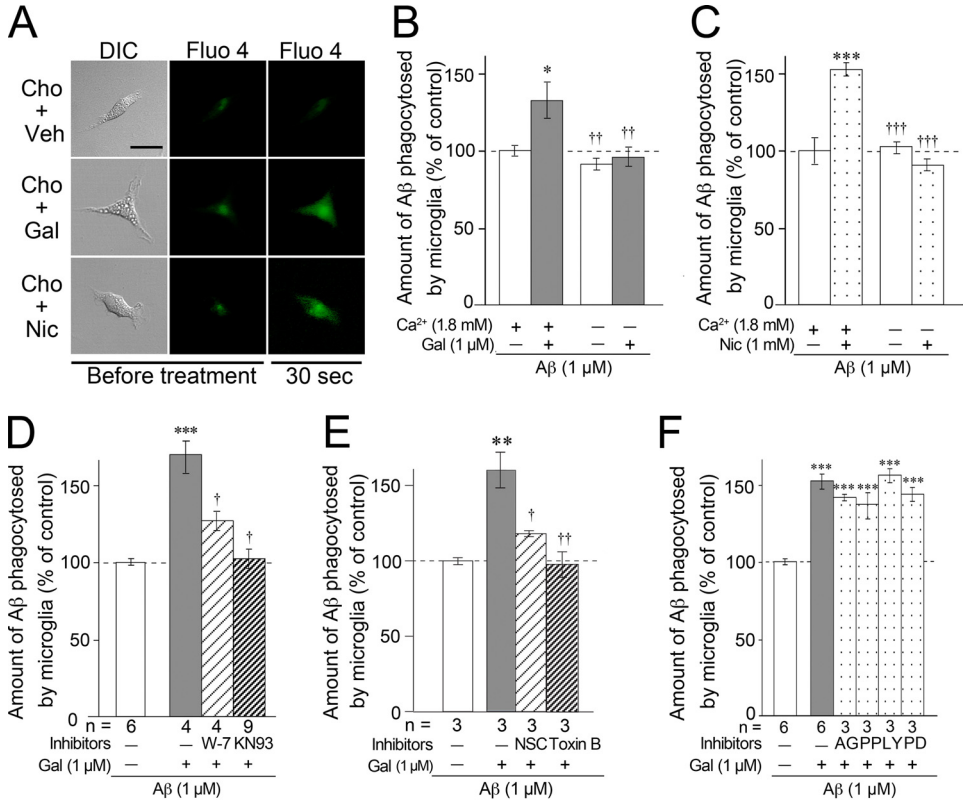

FIGURE 6. **Involvement of Ca^{2+} influx via nAChRs and signaling cascades of CaM-CaMKII and CaM-Rac1 in galantamine-enhanced microglial Aβ phagocytosis.** *A*, time lapse imaging using laser confocal microscopy was examined after pretreatment with Fluo 4-AM. *Scale bar*, 20 μm. *Cho*, choline; *Veh*, vehicle; *Gal*, galantamine; *Nic*, nicotine. *B* and *C*, in Ca^{2+}-free medium supplemented with choline, microglial Aβ phagocytosis was not enhanced by treatment with galantamine (*B*) or nicotine (*C*). *, $p < 0.05$; ***, $p < 0.001$ *versus* Aβ42 alone in Ca^{2+}-containing culture medium. ††, $p < 0.01$; †††, $p < 0.001$ *versus* Aβ42 plus galantamine (*B*) or nicotine (*C*) in Ca^{2+}-containing culture medium. The data represent the means ± S.E. of four samples in each group. *D*, W-7 (an inhibitor of CaM; 20 μM) or KN93 (an inhibitor of CaMKII; 20 μM) was added 10 min before Aβ42 plus galantamine in regular medium containing Ca^{2+} and choline. ***, $p < 0.001$ *versus* Aβ42 alone. †, $p < 0.05$ *versus* Aβ42 plus galantamine. *n*, number of samples. *E*, in regular medium containing Ca^{2+} and choline, NSC23766 (a Rac1-specific inhibitor; 100 μM) or Toxin B (a broad inhibitor of small GTPases; 5 ng/ml) was added 10 min before Aβ42 plus galantamine. **, $p < 0.01$ *versus* Aβ42 alone. †, $p < 0.05$; ††, $p < 0.01$ *versus* Aβ42 plus galantamine. *NSC*, NSC23766. *F*, in regular medium containing Ca^{2+} and choline, microglia were treated with 10 μM AG490, 10 μM PP2, 10 μM LY294002, and 50 μM PD98059, which are inhibitors of JAK2, Fyn, PI3K, and MAPKK, respectively. ***, $p < 0.001$ *versus* Aβ42 alone. *AG*, AG490; *PP*, PP2; *LY*, LY294002; *PD*, PD98059.

tured any remaining Ca^{2+} by adding 0.1 mM EGTA. In the absence of galantamine or nicotine, the levels of microglial Aβ phagocytosis were almost the same in Ca^{2+} (−) DMEM and Ca^{2+} (+) DMEM. Although galantamine (Fig. 6*B*) and nicotine (Fig. 6*C*) significantly enhanced microglial Aβ phagocytosis in Ca^{2+} (+) DMEM, the effect was not observed in Ca^{2+} (−) DMEM. Furthermore, 20 μM W-7 (an inhibitor of calmodulin (CaM)) and 10 μM KN93 (an inhibitor of Ca^{2+}/CaM-dependent protein kinase II (CaMKII)) significantly inhibited galantamine-enhanced microglial Aβ phagocytosis (Fig. 6*D*). This result suggests that Ca^{2+} influx through nAChRs and subsequent activation of CaM-CaMKII signaling cascade are involved in enhanced microglial Aβ phagocytosis.

In platelet, CaM directly binds to Ras-related C3 botulinum toxin substrate 1 (Rac1) in a Ca^{2+}-dependent manner and is involved in Rac1 activation (37). Rac1 is a Rho (Ras homologous) family small GTPase and regulates actin reorganization (38). We next examined the effects of Toxin B (a broad inhibitor of Rho family small GTPases including Rac1) and NSC23766 (a Rac1-specific inhibitor) in Ca^{2+} (+) DMEM containing 28 μM choline. Pretreatment with 5 ng/ml Toxin B and 100 μM NSC23766 significantly inhibited galantamine-enhanced microglial Aβ phagocytosis (Fig. 6*E*). This result suggests that Ca^{2+}-dependent CaM-Rac1 signaling cascade is also involved in galantamine-enhanced microglial Aβ phagocytosis.

Cell signaling cascades such as Janus activated kinase-2 (JAK2)- phosphoinositide-3 kinase (PI3K)-Akt cascade and Fyn-PI3K-Akt cascade have been reported to be involved in neuroprotection conferred by nAChR stimulation in neurons (21, 39). In addition, Fyn generally activates mitogen-activated protein kinase kinase (MAPKK). Consequently, we further investigated whether these cell signaling cascades are involved in galantamine-enhanced microglial Aβ phagocytosis. Microglia were treated with AG490, PP2, LY294002, and PD98059 (inhibitors of JAK2, Fyn, PI3K, and MAPKK, respectively) in Ca^{2+} (+) DMEM containing 28 μM choline, but they did not inhibit galantamine-enhanced Aβ phagocytosis (Fig. 6*F*). These results suggest that rather than JAK2, Fyn, PI3K, or MAPKK, the activation of CaM, CaMKII, and Rac1 by Ca^{2+} influx plays a crucial role in the cell signaling cascades linked to the promotion of microglial Aβ phagocytosis induced by nAChR stimulation.

Effect of Galantamine on Aβ Clearance in Aβ-injected Rat Brain—Subsequently, we investigated the effect of galantamine on *in vivo* Aβ clearance in the rat brain. We first mi-

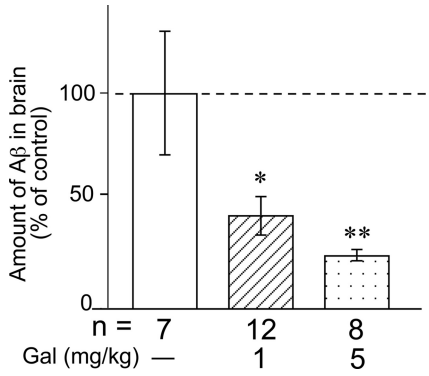

FIGURE 7. **Galantamine increased Aβ clearance in the brains of Aβ-injected rats.** After the subchronic (14 days) intraperitoneal administrations of galantamine (1 or 5 mg/kg), the amount of Aβ in brains of Aβ-injected rats was measured by ELISA. Aβ was undetectable in all Tris-extracted fractions. The amount of Aβ in FA-extracted fractions was significantly reduced by the administration of galantamine in a dose-dependent manner compared with vehicle-treated rats. *, $p < 0.05$; **, $p < 0.01$ *versus* vehicle-treated Aβ-injected rats. *Gal*, galantamine; *n*, number of samples.

croinjected 1 μg of human Aβ42 into the rat hippocampus (~100 mg of wet weight). It is theoretically estimated that 2222 pmol/g of tissue of human Aβ42 existed in the hippocampus immediately after the microinjection. A previous study measured endogenous levels of rat Aβ40 and Aβ42 produced in brains of wild-type rats by ELISA and estimated the concentrations to be ~50 and 13 pmol/g of tissue, respectively (40). It suggests that the endogenous levels of rat Aβ40 and Aβ42 might be ~2.3 and 0.6% of the exogenously microinjected human Aβ42, respectively. In addition, we used a human Aβ42-specific ELISA kit for the measurement of exogenously microinjected human Aβ42 (cross-reactivity: rat Aβ40 ≤ 0.1%, rat Aβ42 ≤ 0.1%). Therefore, we considered that the influence of endogenous Aβ was negligible in the measurement of the exogenously microinjected human Aβ42. In the next step, rats that had received intrahippocampal Aβ42 injection received galantamine (1 or 5 mg/kg) intraperitoneally once daily for 14 consecutive days. As shown in Fig. 7, the amount of Aβ was significantly reduced by galantamine in a dose-dependent manner, compared with the vehicle-treated rats. We previously analyzed that in the Aβ-injected rat brain, microglial Aβ phagocytosis has been proposed to be a major mechanism of Aβ clearance (29). Therefore, this result suggests that galantamine may enhance microglial Aβ phagocytosis and then promote the Aβ clearance from the Aβ-injected rat brain.

Effect of Galantamine on Spatial Learning and Memory and Aβ Clearance in APdE9 Mice—Before the drug treatment, we tested 21 APdE9 mice and 14 nontransgenic littermates in MWM at 9 months of age. In the acquisition trials, no difference was found in swimming speed ($F_{1,66} = 0.32$, $p = 0.5744$). In the escape latency in the acquisition trials, although it was not significant, a weak genotype effect was observed ($F_{1,66} = 3.13$, $p = 0.0863$; Fig. 8*A*). In the probe test, APdE9 mice showed significantly less retention time in the former platform location (target quadrant) than nontransgenic littermates (Fig. 8*C*). These results indicate that APdE9 mice displayed a weak decline in spatial learning and memory at 9 months of age.

Starting at 9 months of age, groups of APdE9 mice were orally administrated 1 or 5 mg/kg of galantamine or 10 ml/kg of PBS once daily for 56 days. Groups of age-matched nontransgenic littermates received 5 mg/kg of galantamine or 10 ml/kg of PBS. Three days before the final drug treatment (at 11 months of age), a second block of acquisition trials and a single probe test were started. In the acquisition trials, no difference was found in swimming speed among all groups ($F_{4,60} = 1.59$, $p = 0.2017$). In the escape latency between vehicle-treated APdE9 mice and vehicle-treated nontransgenic littermates, there was a significant genotype effect ($F_{1,24} = 16.83$, $p = 0.0015$; Fig. 8*B*) in the acquisition trials. In the probe test, vehicle-treated APdE9 mice predictably showed significantly less retention time in the target quadrant than vehicle-treated nontransgenic littermates (Fig. 8*D*). Thus, vehicle-treated APdE9 mice displayed a significant decline in spatial learning and memory at 11 months of age. In the comparison among APdE9 mice, a significant drug effect was detected in the escape latency ($F_{2,36} = 9.37$, $p = 0.0016$; Fig. 8*B*) in the acquisition trials. Post hoc analysis revealed that in the acquisition trials, both low and high doses of galantamine significantly improved the performance in the 11-month-old APdE9 mice. Similarly, in the probe test, galantamine treatment increased retention time, and the performance was significantly improved by treatments of low and high doses of galantamine (Fig. 8*D*). The typical swimming trajectories of the 11-month-old mice are shown in Fig. 8*E*. Thus, galantamine treatment improved behavioral performance on the spatial learning and memory in aged APdE9 mice.

After the MWM experiment, we finally examined the Aβ burden in the brains of APdE9 mice. In the cortices and hippocampi of vehicle-treated APdE9 mice, Aβ plaques were markedly formed (Fig. 9*A*). Moderate accumulations of Aβ were detected in APdE9 mice treated with 5 mg/kg galantamine (Fig. 9*B*). Microglia accumulated on the Aβ plaques in the vehicle-treated (Fig. 9, *C* and *E*) and galantamine-treated (Fig. 9, *D* and *F*) APdE9 mice were expressed in α7 nAChRs (Fig. 9, *C* and *D*) and the APL-binding site (Fig. 9, *E* and *F*). The amounts of Aβ40 (Fig. 9*G*) and Aβ42 (Fig. 9*H*) in brains of APdE9 mice were measured by ELISA. Although the amounts of soluble Aβ40 and Aβ42 in TBS-extracted fractions were almost the same between the drug treatments, those of insoluble Aβ40 and Aβ42 in FA-extracted fractions were significantly decreased by the treatment of galantamine. Thus, in two different models of AD, such as Aβ-injected rats and transgenic mice, galantamine promoted Aβ clearance in their brains.

DISCUSSION

Galantamine has been reported to have multiple actions on neurons. One of the most interesting effects is exerted by AChE inhibition, resulting in enhanced cholinergic neurotransmission caused by the increased acetylcholine level. Another effect is the neuroprotection exerted through allosteric modulation of nAChRs on neurons (21). In the present study, we demonstrated for the first time that galantamine allosterically modulates microglial nAChRs and enhances microglial Aβ phagocytosis. This effect may also contribute to neuropro-

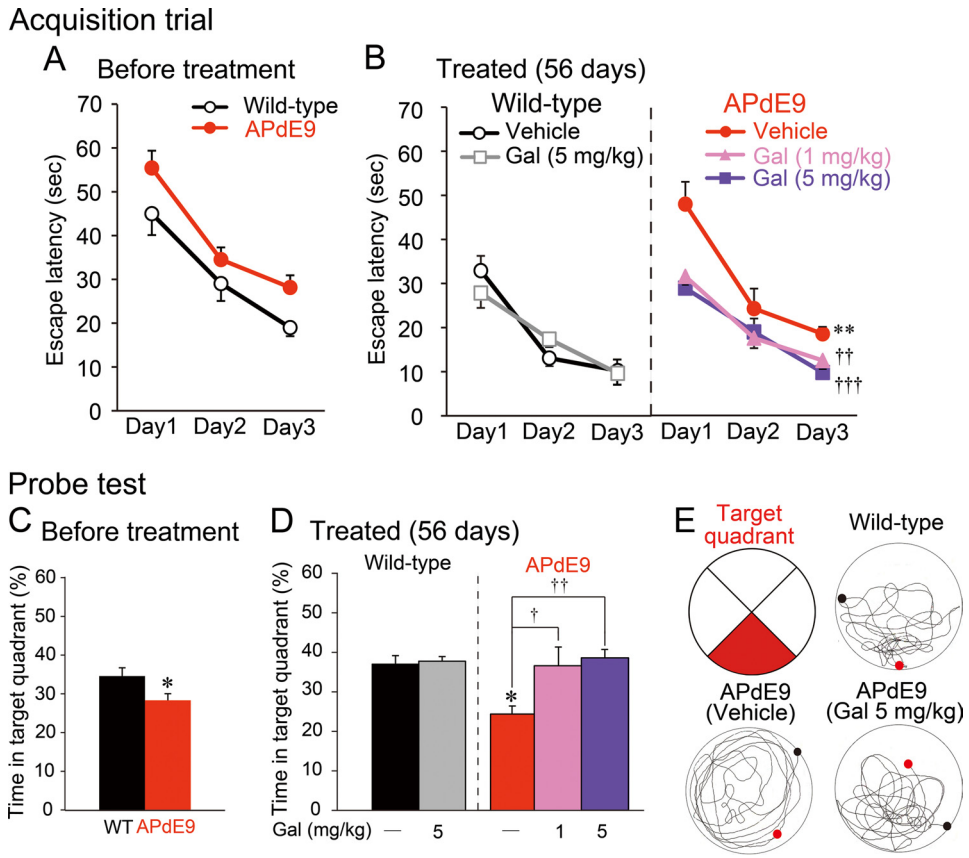

FIGURE 8. **Galantamine improved spatial learning and memory in APdE9 mice.** *A* and *B*, in MWM examination, APdE9 mice and wild-type littermates were given three acquisition trials/day for three consecutive days at 4 days before the drug treatments (*A*) and at 3 days before the final administrations (*B*). Wild-type littermates ($n = 14$) were divided into a vehicle-treated group ($n = 7$) and a 5 mg/kg galantamine-treated group ($n = 7$). APdE9 mice were divided into a vehicle-treated group ($n = 7$), a 1 mg/kg of galantamine-treated group ($n = 7$), and a 5 mg/kg of galantamine-treated group ($n = 7$). **, $p < 0.01$ *versus* vehicle-treated wild-type mice. ††, $p < 0.01$; †††, $p < 0.001$ *versus* vehicle-treated APdE9 mice. *Gal*, galantamine. *C* and *D*, 1 day after the last acquisition trial, a single probe test was conducted for each study subject to measure spatial bias for previous platform location at 4 days before the drug treatments (*C*) and at 3 days before the final administrations (*D*). *, $p < 0.05$ *versus* wild-type mice (*C*) and vehicle-treated wild-type mice (*D*). †, $p < 0.05$; ††, $p < 0.01$ *versus* vehicle-treated APdE9 mice. *E*, the *red area* indicates the target quadrant, and typical swimming trajectories in the last probe test are shown. In each circle, the *black dot* indicates the starting point, and the *red dot* shows the final position of the mouse at the end of the probe test.

tection because neurotoxicity of Aβ has been demonstrated (41, 42), and Aβ-dependent formation (43, 44) and/or maturation (45) of neurofibrillary tangles have been suggested. Therefore, the effect of galantamine on microglia could be related to the long term cognitive benefits of galantamine, as reported in AD patients (16). Thus, we propose a further advantage of galantamine as a therapeutic drug for AD.

In the galantamine-enhanced microglial Aβ phagocytosis, we found that at least two sites on nAChRs, the acetylcholine-binding site (Fig. 2*C*) and the APL-binding site (Fig. 4), contribute. In other words, galantamine may require some natural or acetylcholine competitive agonists to enhance microglial Aβ phagocytosis. Indeed, galantamine utilized choline, an acetylcholine competitive and relatively selective full agonist for α7 nAChRs (33–35), to enhance Aβ phagocytosis (Fig. 5*A*). Furthermore, the concentration-dependent curves of choline and nicotine on microglial Aβ phagocytosis (Fig. 5, *B* and *C*, respectively) revealed that in the absence of galantamine, choline and nicotine at concentrations of ~100 μM and higher enhanced Aβ phagocytosis. On the other hand, 1 μM galantamine dramatically increased choline or nicotine sensitivity of microglial nAChRs, and 1 μM choline or 0.03 μM nicotine was enough to enhance microglial Aβ phagocytosis.

Although further studies are required to clarify the reason why nicotine was more sensitive than choline, galantamine dramatically sensitized microglial nAChRs to choline and nicotine. A previous study measured extracellular choline in the mouse dorsal hippocampus by microdialysis and estimated the concentration to be 4.36 μM (46). These findings suggest that choline alone at a physiological concentration is unlikely to activate nAChRs on microglia in the brain. However, in the presence of galantamine, such a low concentration of choline may suffice to activate nAChRs on microglia and consequently increase microglial Aβ phagocytosis in the brain.

The α7 nAChRs are ion channels with high Ca^{2+} permeability that exhibit a low affinity for nicotine and are desensitized rapidly in neurons (36). In the present study, the influx of extracellular Ca^{2+} (Fig. 6, *A–C*, and supplemental Videos S1–S3) and subsequent activation of the CaM-CaMKII and CaM-Rac1 pathways (Fig. 6, *D* and *E*, respectively) were involved in promoting microglial Aβ phagocytosis. However, Suzuki *et al.* (24) have reported that microglial α7 nAChRs drive a phospholipase C-inositol trisphosphate pathway and elicit Ca^{2+} release from an intracellular Ca^{2+} store. Therefore, the possibility remains that intracellular Ca^{2+} is involved in the activation of the

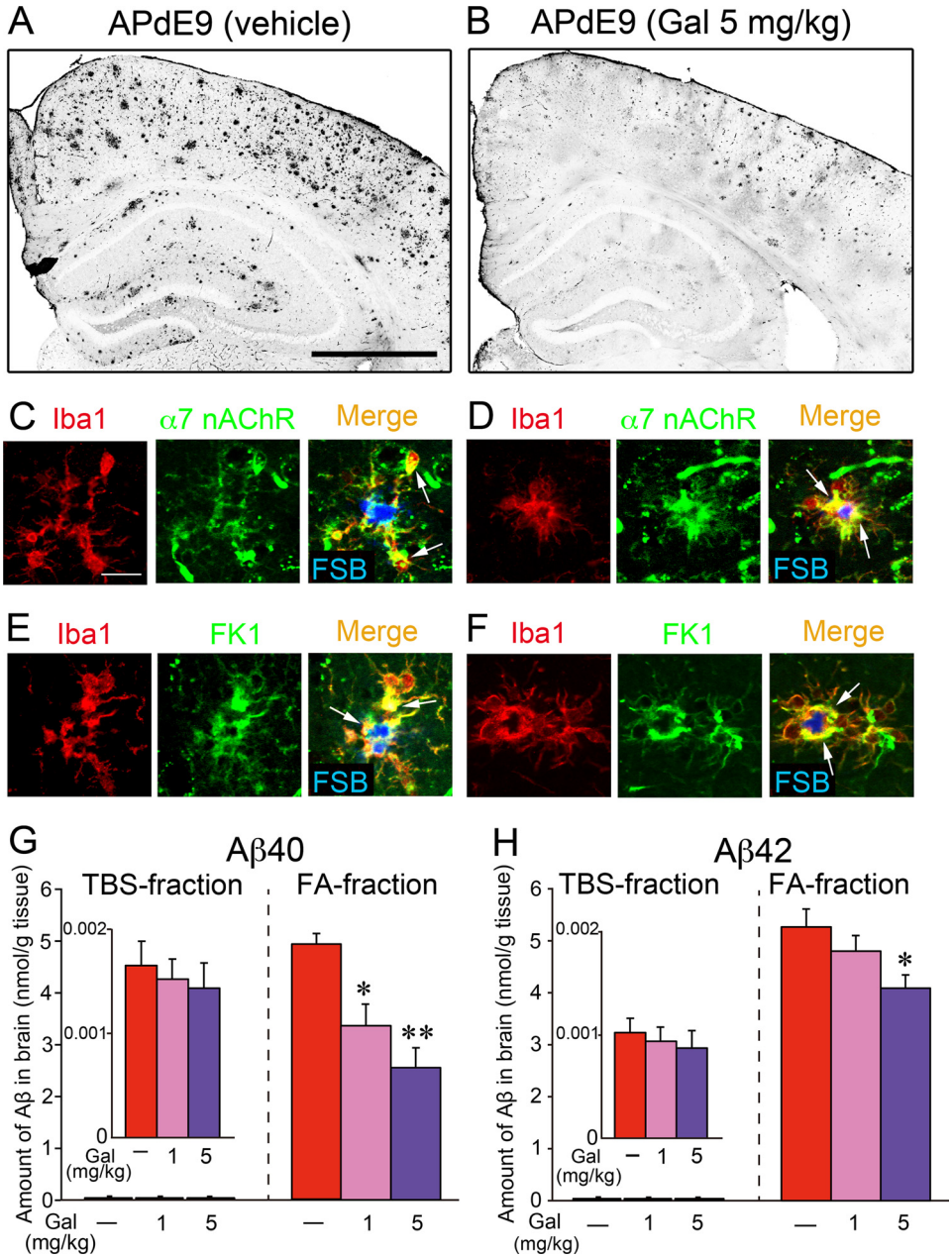

FIGURE 9. **Galantamine increased Aβ clearance in the brains of APdE9 mice.** *A* and *B*, brain sections of vehicle-treated (*A*) or galantamine-treated (*B*) APdE9 mice were immunostained with anti-Aβ antibody. *Scale bar*, 500 μm. *C–F*, in the brains of vehicle-treated (*C* and *E*) and galantamine-treated (*D* and *F*) APdE9 mice, immunoreactivities of α7 nAChRs (*C* and *D*, green) and APL-binding site (*E* and *F*, FK1; green) were co-localized (*arrows*) with microglia (Iba1; *red*) accumulated on Aβ plaque (FSB; *blue*). *Scale bar*, 20 μm. *G* and *H*, in the TBS-extracted fractions and FA-extracted fractions prepared from the brains of APdE9 mice, amounts of Aβ40 (*G*) and Aβ42 (*H*) were measured by ELISA. *, $p < 0.05$; **, $p < 0.01$ *versus* vehicle-treated APdE9 mice. *Gal*, galantamine. The data represent the means ± S.E. of seven samples in each group.

CaM-CaMKII and CaM-Rac1 pathways and galantamine-enhanced microglial Aβ phagocytosis.

In neurons, CaMKII is an abundant synaptic protein that has been shown to regulate bundling of actin filaments leading to structural modifications of synapses (47). At resting synapse, actin filaments are bundled by the nonactivated CaMKII. When CaMKII is activated by neuronal activity and the resultant Ca^{2+} influx, CaMKII detaches from actin filaments and allows actin reorganization by small GTPases. In this study, we also revealed the involvement of Rac1 activity in the galantamine-enhanced microglial Aβ phagocytosis. Rac1 is a small GTPase and regulates actin assembly through the activation of Wiskott-Aldrich syndrome protein family verprolin-homologous protein (WAVE) (48). In addition, we suggested previously that actin reorganization regulated by WAVE participates predominantly in microglial Aβ phagocytosis (28). Based on the evidence presented, we postulate that as downstream mechanisms of Ca^{2+} influx through α7 nAChRs, the activation pathways for the regulation of actin reorganization, such as CaM-CaMKII and CaM-Rac1-WAVE, are critically and simultaneously involved in the galantamine-enhanced microglial Aβ phagocytosis.

In the present study, we were able to clearly demonstrate an increased clearance of Aβ in the brain of Aβ-injected rat

by subchronic (14 days) intraperitoneal administration of galantamine (1 and 5 mg/kg) (Fig. 7). Recent *in vivo* studies using Tg2576 transgenic mice, an animal AD model that develops Aβ plaques in the brain, have revealed that nicotine reduces the brain Aβ level (49, 50). These findings support our hypothesis that modulation of α7 nAChRs by galantamine effectively increased Aβ clearance in Aβ-injected rat brain. However, Unger *et al.* (51) reported that subchronic subcutaneous treatment with galantamine (2 mg/kg) in Tg2576 mice had no effect on brain Aβ levels. It is possible that the duration of galantamine treatment (10 days) was not long enough to detect a difference in brain Aβ levels, because a massive amount of Aβ is continuously produced in aged Tg2576 mice. Therefore, we further investigated whether the chronic (56 days) administration of galantamine to a transgenic mouse model of AD (APdE9 mouse) is effective on the Aβ clearance in the brain. Indeed, the chronic treatment of galantamine improved the impaired spatial learning and memory in aged APdE9 mice (Fig. 8) and significantly reduced amounts of Aβ in FA-extracted fractions prepared from the brains of APdE9 mice (Fig. 9). These data suggest that the promotion of Aβ clearance in the brains of Aβ-injected rats and APdE9 mice may be induced by galantamine treatment through the enhancement of microglial Aβ phagocytosis as shown in the study of primary-cultured rat microglia (Fig. 2*A*). We further speculate that the long term clinical treatment of galantamine to patients with AD may also give rise to a promotional effect on the Aβ clearance through the microglial Aβ phagocytosis, and this effect of galantamine on microglia may, at least partially, contribute to its long lasting cognitive benefits revealed in the latest clinical trial (16).

A recent long term follow-up study of patients with AD who were immunized with Aβ42 peptide (AN1792) suggested that the immunization is associated with a reduction in fibrillar Aβ plaques (52). Unfortunately, this study could not detect the inhibitory effect on the time to severe dementia in the AN1792 group compared with the placebo group. Thus, this study also suggested a necessity of the immunization as early as possible. In addition, anti-Aβ antibody produced by the immunization with Aβ peptides induced not only microglial Aβ phagocytosis and drainage of brain Aβ into systemic circulation but also disaggregation of fibrillar Aβ (53). Therefore, another possible explanation for follow-up study results is that immunization failed to reduce the concentration of oligomeric Aβ, a synaptotoxic form of Aβ (54), and might even have increased it during the active phase of disaggregation of fibrillar Aβ plaques (55). Microglia phagocytose and degrade oligomeric Aβ (56). In the present study, although we could not detect a significant reduction of Aβ in the TBS-extracted fractions, the amounts of Aβ were not increased by the treatment of galantamine to APdE9 mice. Therefore, enhanced microglial Aβ phagocytosis by galantamine may exert Aβ clearance from brains barring diffusion of toxic oligomeric Aβ.

In conclusion, we have provided new evidence that modulation of microglial nAChRs by galantamine or stimulation of nAChRs by nicotine enhances Aβ phagocytosis in primary-cultured rat microglia. Galantamine sensitizes microglial nAChRs to choline and nicotine by binding to the APL-binding site on nAChRs. Thus, galantamine requires extracellular choline or other acetylcholine competitive agonists to enhance microglial Aβ phagocytosis. Nicotine alone directly induces enhanced microglial Aβ phagocytosis. Furthermore, we also suggest that the Ca^{2+} signaling cascade followed by CaM-CaMKII and CaM-Rac1 pathways for the regulation of actin reorganization may be involved in the phagocytic enhancement in microglia. Subsequently, we postulate that this mechanism may also be involved in galantamine-enhanced Aβ clearance observed in the brains of Aβ-injected rats and APdE9 mice. All of the results presented here suggest a further advantage of galantamine as a therapeutic drug for AD and significant therapeutic potential of microglial nAChRs, such as α7 nAChRs, in the treatment of AD.

REFERENCES

1. Selkoe, D. J. (1999) *Nature* **399,** A23–31
2. Hardy, J., and Selkoe, D. J. (2002) *Science* **297,** 353–356
3. Schenk, D., Barbour, R., Dunn, W., Gordon, G., Grajeda, H., Guido, T., Hu, K., Huang, J., Johnson-Wood, K., Khan, K., Kholodenko, D., Lee, M., Liao, Z., Lieberburg, I., Motter, R., Mutter, L., Soriano, F., Shopp, G., Vasquez, N., Vandevert, C., Walker, S., Wogulis, M., Yednock, T., Games, D., and Seubert, P. (1999) *Nature* **400,** 173–177
4. Janus, C., Pearson, J., McLaurin, J., Mathews, P. M., Jiang, Y., Schmidt, S. D., Chishti, M. A., Horne, P., Heslin, D., French, J., Mount, H. T., Nixon, R. A., Mercken, M., Bergeron, C., Fraser, P. E., St George-Hyslop, P., and Westaway, D. (2000) *Nature* **408,** 979–982
5. Morgan, D., Diamond, D. M., Gottschall, P. E., Ugen, K. E., Dickey, C., Hardy, J., Duff, K., Jantzen, P., DiCarlo, G., Wilcock, D., Connor, K., Hatcher, J., Hope, C., Gordon, M., and Arendash, G. W. (2000) *Nature* **408,** 982–985
6. Bard, F., Cannon, C., Barbour, R., Burke, R. L., Games, D., Grajeda, H., Guido, T., Hu, K., Huang, J., Johnson-Wood, K., Khan, K., Kholodenko, D., Lee, M., Lieberburg, I., Motter, R., Nguyen, M., Soriano, F., Vasquez, N., Weiss, K., Welch, B., Seubert, P., Schenk, D., and Yednock, T. (2000) *Nat. Med.* **6,** 916–919
7. Takata, K., Hirata-Fukae, C., Becker, A. G., Chishiro, S., Gray, A. J., Nishitomi, K., Franz, A. H., Sakaguchi, G., Kato, A., Mattson, M. P., Laferla, F. M., Aisen, P. S., Kitamura, Y., and Matsuoka, Y. (2007) *Eur. J. Neurosci.* **26,** 2458–2468
8. Nicoll, J. A., Wilkinson, D., Holmes, C., Steart, P., Markham, H., and Weller, R. O. (2003) *Nat. Med.* **9,** 448–452
9. Davies, P., and Maloney, A. J. (1976) *Lancet* **2,** 1403
10. Whitehouse, P. J., Price, D. L., Clark, A. W., Coyle, J. T., and DeLong, M. R. (1981) *Ann. Neurol.* **10,** 122–126
11. Whitehouse, P. J., Price, D. L., Struble, R. G., Clark, A. W., Coyle, J. T., and Delon, M. R. (1982) *Science* **215,** 1237–1239
12. Coyle, J. T., Price, D. L., and DeLong, M. R. (1983) *Science* **219,** 1184–1190
13. Raskind, M. A., Peskind, E. R., Wessel, T., and Yuan, W. (2000) *Neurology* **54,** 2261–2268
14. Raskind, M. A., and Peskind, E. R. (2001) *Med. Clin. North Am.* **85,** 803–817
15. Raskind, M. A. (2003) *Neurologist* **9,** 235–240
16. Raskind, M. A., Peskind, E. R., Truyen, L., Kershaw, P., and Damaraju, C. V. (2004) *Arch. Neurol.* **61,** 252–256
17. Maelicke, A., Coban, T., Storch, A., Schrattenholz, A., Pereira, E. F., and Albuquerque, E. X. (1997) *J. Recept. Signal Transduct. Res.* **17,** 11–28
18. Maelicke, A., and Albuquerque, E. X. (2000) *Eur. J. Pharmacol.* **393,** 165–170
19. Maelicke, A., Samochocki, M., Jostock, R., Fehrenbacher, A., Ludwig, J., Albuquerque, E. X., and Zerlin, M. (2001) *Biol. Psychiatry* **49,** 279–288
20. Samochocki, M., Höffle, A., Fehrenbacher, A., Jostock, R., Ludwig, J., Christner, C., Radina, M., Zerlin, M., Ullmer, C., Pereira, E. F., Lübbert,

H., Albuquerque, E. X., and Maelicke, A. (2003) *J. Pharmacol. Exp. Ther.* **305,** 1024–1036
21. Kihara, T., Sawada, H., Nakamizo, T., Kanki, R., Yamashita, H., Maelicke, A., and Shimohama, S. (2004) *Biochem. Biophys. Res. Commun.* **325,** 976–982
22. Yanagida, T., Takeuchi, H., Kitamura, Y., Takata, K., Minamino, H., Shibaike, T., Tsushima, J., Kishimoto, K., Yasui, H., Taniguchi, T., and Shimohama, S. (2008) *Neurosci. Res.* **62,** 254–261
23. Shytle, R. D., Mori, T., Townsend, K., Vendrame, M., Sun, N., Zeng, J., Ehrhart, J., Silver, A. A., Sanberg, P. R., and Tan, J. (2004) *J. Neurochem.* **89,** 337–343
24. Suzuki, T., Hide, I., Matsubara, A., Hama, C., Harada, K., Miyano, K., Andrä, M., Matsubayashi, H., Sakai, N., Kohsaka, S., Inoue, K., and Nakata, Y. (2006) *J. Neurosci. Res.* **83,** 1461–1470
25. Schrattenholz, A., Godovac-Zimmermann, J., Schäfer, H. J., Albuquerque, E. X., and Maelicke, A. (1993) *Eur. J. Biochem.* **216,** 671–677
26. Schröder, B., Reinhardt-Maelicke, S., Schrattenholz, A., McLane, K. E., Kretschmer, A., Conti-Tronconi, B. M., and Maelicke, A. (1994) *J. Biol. Chem.* **269,** 10407–10416
27. Kakimura, J., Kitamura, Y., Takata, K., Umeki, M., Suzuki, S., Shibagaki, K., Taniguchi, T., Nomura, Y., Gebicke-Haerter, P. J., Smith, M. A., Perry, G., and Shimohama, S. (2002) *FASEB J.* **16,** 601–603
28. Kitamura, Y., Shibagaki, K., Takata, K., Tsuchiya, D., Taniguchi, T., Gebicke-Haerter, P. J., Miki, H., Takenawa, T., and Shimohama, S. (2003) *J. Pharmacol. Sci.* **92,** 115–123
29. Takata, K., Kitamura, Y., Tsuchiya, D., Kawasaki, T., Taniguchi, T., and Shimohama, S. (2004) *J. Neurosci. Res.* **78,** 880–891
30. Jankowsky, J. L., Fadale, D. J., Anderson, J., Xu, G. M., Gonzales, V., Jenkins, N. A., Copeland, N. G., Lee, M. K., Younkin, L. H., Wagner, S. L., Younkin, S. G., and Borchelt, D. R. (2004) *Hum. Mol. Genet.* **13,** 159–170
31. Sala, C., Kimura, I., Santoro, G., Kimura, M., and Fumagalli, G. (1996) *Neurosci. Lett.* **215,** 71–74
32. Schrattenholz, A., Pereira, E. F., Roth, U., Weber, K. H., Albuquerque, E. X., and Maelicke, A. (1996) *Mol. Pharmacol.* **49,** 1–6
33. Mandelzys, A., De Koninck, P., and Cooper, E. (1995) *J. Neurophysiol.* **74,** 1212–1221
34. Papke, R. L., Bencherif, M., and Lippiello, P. (1996) *Neurosci. Lett.* **213,** 201–204
35. Alkondon, M., Pereira, E. F., Cortes, W. S., Maelicke, A., and Albuquerque, E. X. (1997) *Eur. J. Neurosci.* **9,** 2734–2742
36. Cordero-Erausquin, M., Marubio, L. M., Klink, R., and Changeux, J. P. (2000) *Trends Pharmacol. Sci.* **21,** 211–217
37. Elsaraj, S. M., and Bhullar, R. P. (2008) *Biochim. Biophys. Acta* **1783,** 770–778
38. Hall, A. (1998) *Science* **279,** 509–514
39. Kihara, T., Shimohama, S., Sawada, H., Honda, K., Nakamizo, T., Shibasaki, H., Kume, T., and Akaike, A. (2001) *J. Biol. Chem.* **276,** 13541–13546
40. Ramsden, M., Nyborg, A. C., Murphy, M. P., Chang, L., Stanczyk, F. Z., Golde, T. E., and Pike, C. J. (2003) *J. Neurochem.* **87,** 1052–1055
41. Yankner, B. A., Dawes, L. R., Fisher, S., Villa-Komaroff, L., Oster-Granite, M. L., and Neve, R. L. (1989) *Science* **245,** 417–420
42. Yankner, B. A., Duffy, L. K., and Kirschner, D. A. (1990) *Science* **250,** 279–282
43. Götz, J., Chen, F., van Dorpe, J., and Nitsch, R. M. (2001) *Science* **293,** 1491–1495
44. Lewis, J., Dickson, D. W., Lin, W. L., Chisholm, L., Corral, A., Jones, G., Yen, S. H., Sahara, N., Skipper, L., Yager, D., Eckman, C., Hardy, J., Hutton, M., and McGowan, E. (2001) *Science* **293,** 1487–1491
45. Takata, K., Kitamura, Y., Nakata, Y., Matsuoka, Y., Tomimoto, H., Taniguchi, T., and Shimohama, S. (2009) *Am. J. Pathol.* **175,** 17–24
46. Hartmann, J., Kiewert, C., Duysen, E. G., Lockridge, O., and Klein, J. (2008) *Neurochem. Int.* **52,** 972–978
47. Okamoto, K., Narayanan, R., Lee, S. H., Murata, K., and Hayashi, Y. (2007) *Proc. Natl. Acad. Sci. U.S.A.* **104,** 6418–6423
48. Miki, H., Suetsugu, S., and Takenawa, T. (1998) *EMBO J.* **17,** 6932–6941
49. Nordberg, A., Hellström-Lindahl, E., Lee, M., Johnson, M., Mousavi, M., Hall, R., Perry, E., Bednar, I., and Court, J. (2002) *J. Neurochem.* **81,** 655–658
50. Hellström-Lindahl, E., Court, J., Keverne, J., Svedberg, M., Lee, M., Marutle, A., Thomas, A., Perry, E., Bednar, I., and Nordberg, A. (2004) *Eur. J. Neurosci.* **19,** 2703–2710
51. Unger, C., Svedberg, M. M., Yu, W. F., Hedberg, M. M., and Nordberg, A. (2006) *J. Pharmacol. Exp. Ther.* **317,** 30–36
52. Holmes, C., Boche, D., Wilkinson, D., Yadegarfar, G., Hopkins, V., Bayer, A., Jones, R. W., Bullock, R., Love, S., Neal, J. W., Zotova, E., and Nicoll, J. A. (2008) *Lancet* **372,** 216–223
53. Wisniewski, T., and Konietzko, U. (2008) *Lancet Neurol.* **7,** 805–811
54. Walsh, D. M., Klyubin, I., Fadeeva, J. V., Cullen, W. K., Anwyl, R., Wolfe, M. S., Rowan, M. J., and Selkoe, D. J. (2002) *Nature* **416,** 535–539
55. Patton, R. L., Kalback, W. M., Esh, C. L., Kokjohn, T. A., Van Vickle, G. D., Luehrs, D. C., Kuo, Y. M., Lopez, J., Brune, D., Ferrer, I., Masliah, E., Newel, A. J., Beach, T. G., Castaño, E. M., and Roher, A. E. (2006) *Am. J. Pathol.* **169,** 1048–1063
56. Shimizu, E., Kawahara, K., Kajizono, M., Sawada, M., and Nakayama, H. (2008) *J. Immunol.* **181,** 6503–6513